Phosphorylation of MCAD selectively rescues *PINK1* deficiencies in behavior and metabolism

Meredith M. Course[a,b], Anna I. Scott[c], Carmen Schoor[d], Chung-Han Hsieh[a], Amanda M. Papakyrikos[a,e], Dominic Winter[d], Tina M. Cowan[c], and Xinnan Wang[a,*]

[a]Department of Neurosurgery, [b]Neurosciences Graduate Program, [c]Department of Pathology, and [e]Developmental Biology Graduate Program, Stanford University, Stanford, CA 94305; [d]Institute for Biochemistry and Molecular Biology, University of Bonn, 53115 Bonn, Germany

ABSTRACT PTEN-induced putative kinase 1 (PINK1) is a mitochondria-targeted kinase whose mutations are a cause of Parkinson's disease. We set out to better understand PINK1's effects on mitochondrial proteins in vivo. Using an unbiased phosphoproteomic screen in *Drosophila*, we found that PINK1 mediates the phosphorylation of MCAD, a mitochondrial matrix protein critical to fatty acid metabolism. By mimicking phosphorylation of this protein in a *PINK1* null background, we restored *PINK1* null's climbing, flight, thorax, and wing deficiencies. Owing to MCAD's role in fatty acid metabolism, we examined the metabolic profile of *PINK1* null flies, where we uncovered significant disruptions in both acylcarnitines and amino acids. Some of these disruptions were rescued by phosphorylation of MCAD, consistent with MCAD's rescue of *PINK1* null's organismal phenotypes. Our work validates and extends the current knowledge of PINK1, identifies a novel function of MCAD, and illuminates the need for and effectiveness of metabolic profiling in models of neurodegenerative disease.

INTRODUCTION

PTEN-induced putative kinase 1 (PINK1) is a mitochondria-targeted serine/threonine kinase that mediates several pathways to maintain mitochondrial health and function. When mitochondria are damaged or under stress, PINK1 is stabilized on the outer mitochondrial membrane where it phosphorylates its substrates to initiate mitochondrial clearance via mitophagy (Narendra *et al.*, 2008, 2010; Zhou *et al.*, 2008; Whitworth and Pallanck, 2009; Geisler *et al.*, 2010; Vives-Bauza and Przedborski, 2011; Wang *et al.*, 2011; Kondapalli *et al.*, 2012; Chen and Dorn, 2013; Kane *et al.*, 2014; Kazlauskaite *et al.*, 2014; Koyano *et al.*, 2014; Whitworth and Pallanck, 2017). PINK1 also affects mitochondrial

morphology by interacting with fission-and-fusion machinery and promotes the activity of complex I in the electron transport chain (Poole *et al.*, 2008, 2010; Yang *et al.*, 2008; Ziviani *et al.*, 2010; Liu *et al.*, 2011; Vilain *et al.*, 2012; Vos *et al.*, 2012, 2017; Morais *et al.*, 2014; Pogson *et al.*, 2014; Gehrke *et al.*, 2015). The loss of PINK1 in flies leads to a host of phenotypes, including compromised climbing and flight ability, deformed thoraxes, drooped/held-up wings, and reduced ATP production (Clark *et al.*, 2006; Park *et al.*, 2006; Yang *et al.*, 2006). In humans, mutations in *PINK1* underlie some cases of recessive early-onset Parkinson's disease (Valente *et al.*, 2004a,b). Thus, PINK1 plays a critical role in mitochondrial homeostasis, and its disruption has severe effects at the cellular and organismal level.

Of a mitochondrion's myriad responsibilities, its most vital is the production of energy through metabolism, including fatty acid and amino acid metabolism. Fatty acids are broken down by β-oxidation and ultimately generate the most energy per gram of any metabolite. While amino acids do not deliver as much energy per gram as fatty acids, their metabolism boasts the widest variety of pathways. Inborn errors of either fatty acid metabolism or amino acid metabolism can have devastating consequences, including early childhood death (Rinaldo *et al.*, 2002; Wu, 2009; Houten *et al.*, 2016), which illustrates how critical these processes are to cell survival.

We show here that in addition to its other mitochondrial functions, *PINK1* plays a role in fatty acid and amino acid metabolism. We find that an enzyme critical to fatty acid β-oxidation, medium-chain acyl-coenzyme A dehydrogenase (MCAD), is phosphorylated in a PINK1-dependent manner. MCAD's canonical function is to break down medium-chain fatty acids (C6-12), and its deficiency is the most common inborn error of β-oxidation in humans (Rinaldo *et al.*, 2002). Mimicking phosphorylation of MCAD in *PINK1* null flies rescues the flies' deformed thoraxes, drooped/held-up wings, and flight and climbing deficiencies. We also show that the loss of PINK1 leads to substantial disruptions in both acylcarnitines and amino acids and that mimicking phosphorylation of MCAD rescues some of these disruptions.

RESULTS

Phosphorylation of MCAD S347 is dependent on *PINK1* in *Drosophila*

To identify potential novel targets of PINK1, we conducted an unbiased proteomic screen for phosphorylated residues in the mitochondrial fractions of *PINK1* null flies and their genetic controls (Supplemental Figure S1) (Clark *et al.*, 2006). Since PINK1 is a serine/threonine kinase, we searched for phosphorylated peptides whose abundances were decreased with the loss of PINK1. One phosphopeptide of Marf (the *Drosophila* homologue of mitofusin) was dramatically decreased in *PINK1* null flies (Supplemental Figure S2 and Supplemental Table S1). This finding indicates that Marf phosphorylation is dependent on PINK1 in vivo and supports previous findings in multiple systems that Marf/mitofusin is a target of PINK1 (Poole *et al.*, 2008, 2010; Yang *et al.*, 2008; Tanaka *et al.*, 2010; Chen and Dorn, 2013).

In addition to the Marf phosphopeptide, we identified another phosphopeptide with considerably lower abundance in *PINK1* null flies. This phosphopeptide belongs to MCAD, an enzyme critical to the oxidation of medium-chain fatty acids (Rinaldo *et al.*, 2002; Houten *et al.*, 2016). The abundance of this phosphopeptide was reduced in *PINK1* null flies to 12.4% of the level found in controls, while the abundance of another detected unphosphorylated MCAD peptide remained the same in both genotypes (Figure 1A and Supplemental Figure S2). Within the identified phosphopeptide, there was one serine site with a high probability of phosphorylation, verified by manual analysis of the MS/MS spectrum: serine 347 (Supplemental Figure S3 and Supplemental Table S1). This serine site is functionally conserved across species and correlates to threonine 351 in mammals (Figure 1B). Phosphorylation of this site was previously confirmed in humans and mice (Possemato, 2010; Grimsrud *et al.*, 2012; Mulhern, 2012; Humphrey *et al.*, 2013; Bian *et al.*, 2014).

Since MCAD S347 phosphopeptide abundance followed the same pattern as a known PINK1 substrate, Marf, we hypothesized that PINK1 mediates the phosphorylation of MCAD at serine 347. We confirmed that PINK1 can directly phosphorylate MCAD by coupling an in vitro PINK1 kinase assay with Phos-tag acrylamide analysis—Phos-tag ligands bind phosphorylated proteins and slow their migration. We used bacterially expressed *Tribolium castaneum* PINK1 (TcPINK1), which remains active in vitro (Woodroof *et al.*, 2011), and human MCAD (Figure 1C). Collectively, we have provided evidence that PINK1 mediates the phosphorylation of MCAD both in vivo and in vitro.

Generating phosphoresistant and phosphomimetic MCAD S347 transgenic flies

Because phosphorylation of MCAD S347 is reduced in *PINK1* null flies, we reasoned that mimicking phosphorylation at this site could rescue some of *PINK1* null's phenotypes. To test this hypothesis, we generated flies carrying wild-type (Ser347), phosphoresistant (Ser-347Ala), and two phosphomimetic (Ser347Asp, Ser347AspAsp) MCAD transgenes downstream of an upstream activation sequence (UAS). We refer to these transgenes as MCAD (WT), MCAD (A), MCAD (D), and MCAD (DD), respectively (Figure 1D). We used two different phosphomimetic transgenes since it has been observed that sometimes a pair of acidic amino acids serves as a better mimic of phosphorylation than a lone acidic amino acid (Strickfaden *et al.*, 2007; Pearlman *et al.*, 2011). We also included a V5 tag at the C-terminal of these transgenes, so that we could evaluate their expression levels. All transgenes were inserted into the same genomic site using the PhiC31 integrase-mediated transgenesis system to ensure that they had the same genomic regulation (Bischof *et al.*, 2007; Markstein *et al.*, 2008).

To determine that neither the V5 tag nor the phosphorylation state affected localization of MCAD, we probed mitochondrial and cytosolic fractions of fly lysates for both endogenous and transgenic MCAD expression. We verified that an MCAD antibody generated against mammalian MCAD recognized endogenous fly MCAD (Supplemental Figure S4A) using MCAD deficient flies (described later). All V5-tagged MCAD transgenes were expressed at similar levels when driven by the ubiquitous Actin5C-GAL4 driver (Brand and Perrimon, 1993) (Figure 1E, V5 blot), and their expression levels were comparable to those of endogenous MCAD (Figure 1E, MCAD blot). Neither the V5 tag nor the phosphorylation states of the transgenes affected their localization, and both endogenous and transgenic MCAD protein localized to the mitochondria as well as the cytosol, consistent with a previous report in mammals (Du *et al.*, 2013) (Figure 1E).

We then expressed these transgenic forms of MCAD in *PINK1* null flies carrying Actin5C-GAL4 (Park *et al.*, 2006). Importantly, we crossed our *PINK1^null^; Actin5C-GAL4* flies with flies carrying the same attP40 landing site into which the MCAD transgenes were integrated to eliminate bias caused by differing genetic backgrounds. The protein expression levels of all transgenes were comparable, including in a *PINK1* null background (Supplemental Figure S4, B and C). Thus, these transgenes allowed us to observe the effects of mimicking phosphorylation of MCAD S347 in a *PINK1* null background, while controlling for any other genetic factors.

Phosphomimetic MCAD S347 rescues behavioral and morphological deficiencies in *PINK1* null flies

We first used these wild-type, phosphoresistant, and phosphomimetic MCAD transgenic flies to determine whether mimicking phosphorylation at MCAD S347 could rescue either of *PINK1* null's established climbing and flight phenotypes (Clark *et al.*, 2006; Park *et al.*, 2006). Our *PINK1* null flies took significantly longer to climb 8 cm than control flies, and this climbing latency was fully rescued by MCAD (D) and MCAD (DD), partially rescued by MCAD (WT), and not rescued by MCAD (A). Notably, MCAD (D) and MCAD (DD) rescued the phenotype significantly better than MCAD (WT) (Figure 2A). Our *PINK1* null flies also exhibited a striking flight deficit—~80% were unable to fly—which was significantly rescued by MCAD (D) and MCAD (DD) and not rescued by MCAD (A) or MCAD (WT) (Figure 2B). Thus, mimicking phosphorylation of MCAD at serine 347 rescued *PINK1* null's climbing and flight deficits.

We next explored whether phosphomimetic MCAD could rescue either of *PINK1* null's established indented thorax or drooped/held-up wing phenotypes (Clark *et al.*, 2006; Park *et al.*, 2006). We observed that ~65% of our *PINK1* null flies displayed indented thoraxes, which are indicative of muscle degeneration (Clark *et al.*, 2006; Park *et al.*, 2006). This number was significantly
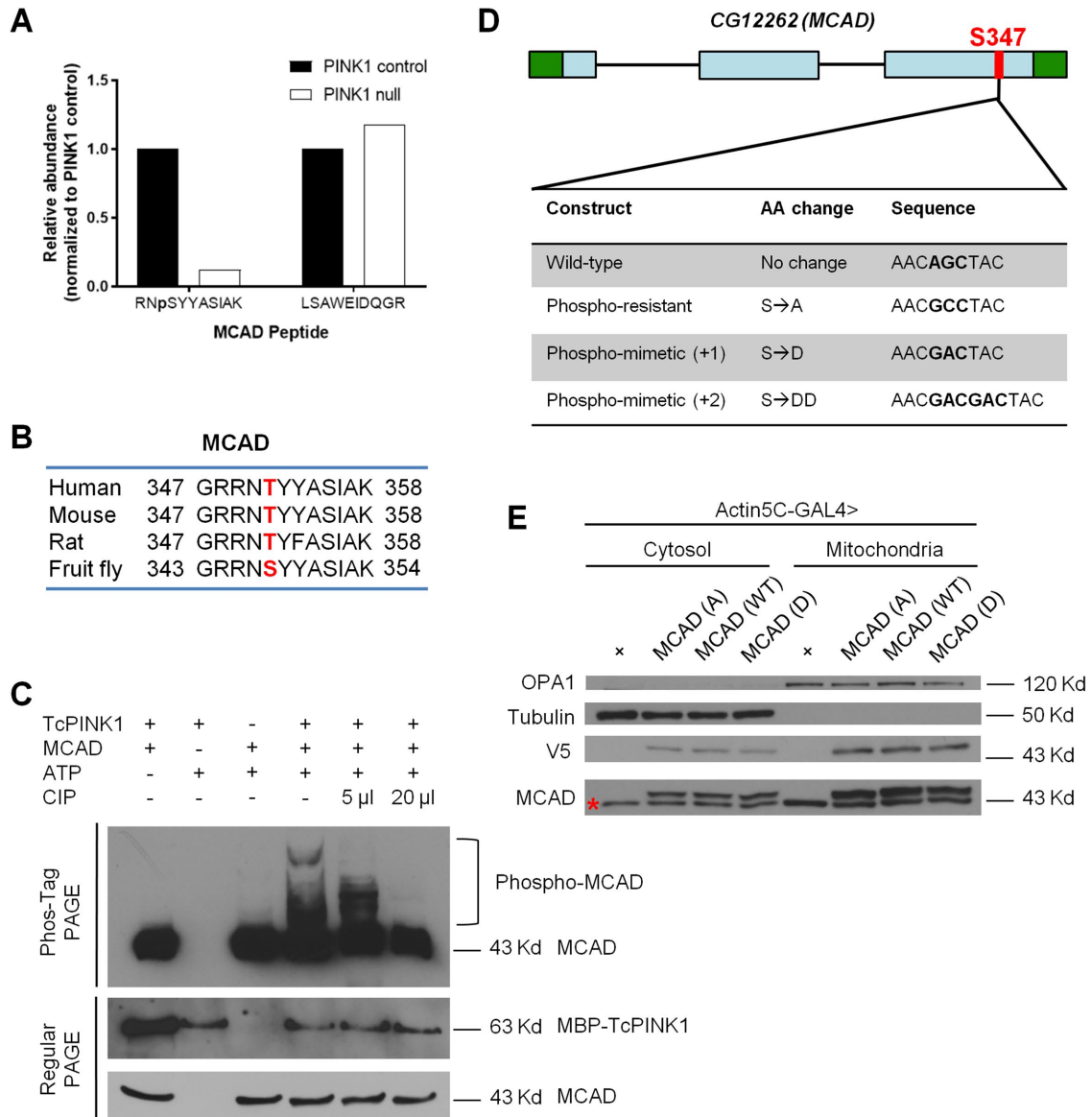
FIGURE 1: Phosphorylation of MCAD S347 is dependent on *PINK1* in *Drosophila*. (A) Phosphopeptide analysis showing relative levels of phosphorylated (left) and unphosphorylated (right) MCAD peptide in mitochondrial fractions from 5-d-old control and *PINK1* null male flies. (B) Sequence alignment of human, mouse, rat, and fly *MCAD*. S347/T351 is marked in red. (C) Phos-tag and regular PAGE gels showing in vitro kinase assay for MCAD and TcPINK1. Phos-tag gel is probed with anti-MCAD to detect both unphosphorylated and the slower-migrating phosphorylated MCAD. Regular PAGE gels are probed with anti-MCAD and anti-MBP to detect MCAD and TcPINK1, respectively, in the in vitro kinase assays. CIP is calf intestinal alkaline phosphatase. The same results were repeated three times (D) Schematic depiction of *Drosophila* gene *CG12262* (*MCAD*) detailing sequences used to generate wild-type, phosphoresistant and phosphomimetic S347. Green boxes are 5′ and 3′ UTRs; blue boxes are exons. (E) Representative Western blot of mitochondrial and cytosolic fractions from *Actin5C-GAL4* alone (control) and *Actin5C-GAL4* driving MCAD (A), MCAD (WT), and MCAD (D) transgenic constructs. Samples were probed with anti-tubulin as a cytosolic loading control, anti-OPA1 as a mitochondrial loading control, anti-MCAD to identify endogenous and transgenic localization, and anti-V5 to verify transgenic localization. Note that endogenous MCAD (red asterisk) migrates faster than V5-tagged MCAD in the anti-MCAD blot. The slightly shifted V5-tagged transgenes are verified in the separate anti-V5 blot. $n = 25$ flies lysed per sample for each experiment; three biological replicates per genotype.

decreased by expression of MCAD (D) and MCAD (DD) and not by expression of MCAD (A) or MCAD (WT) (Figure 2, C and E). Similarly, we found that ~40% of our *PINK1* null flies exhibited drooped or held-up wings. This number was significantly decreased by expression of MCAD (D), and not by expression of MCAD (A) or MCAD (WT). Rescue by MCAD (DD) did not reach significance, but MCAD (D) and MCAD (DD) were not significantly different (Figure 2, D and F). Overall, mimicking phosphorylation at MCAD S347 significantly improved *PINK1* null's thorax and wing posture phenotypes.
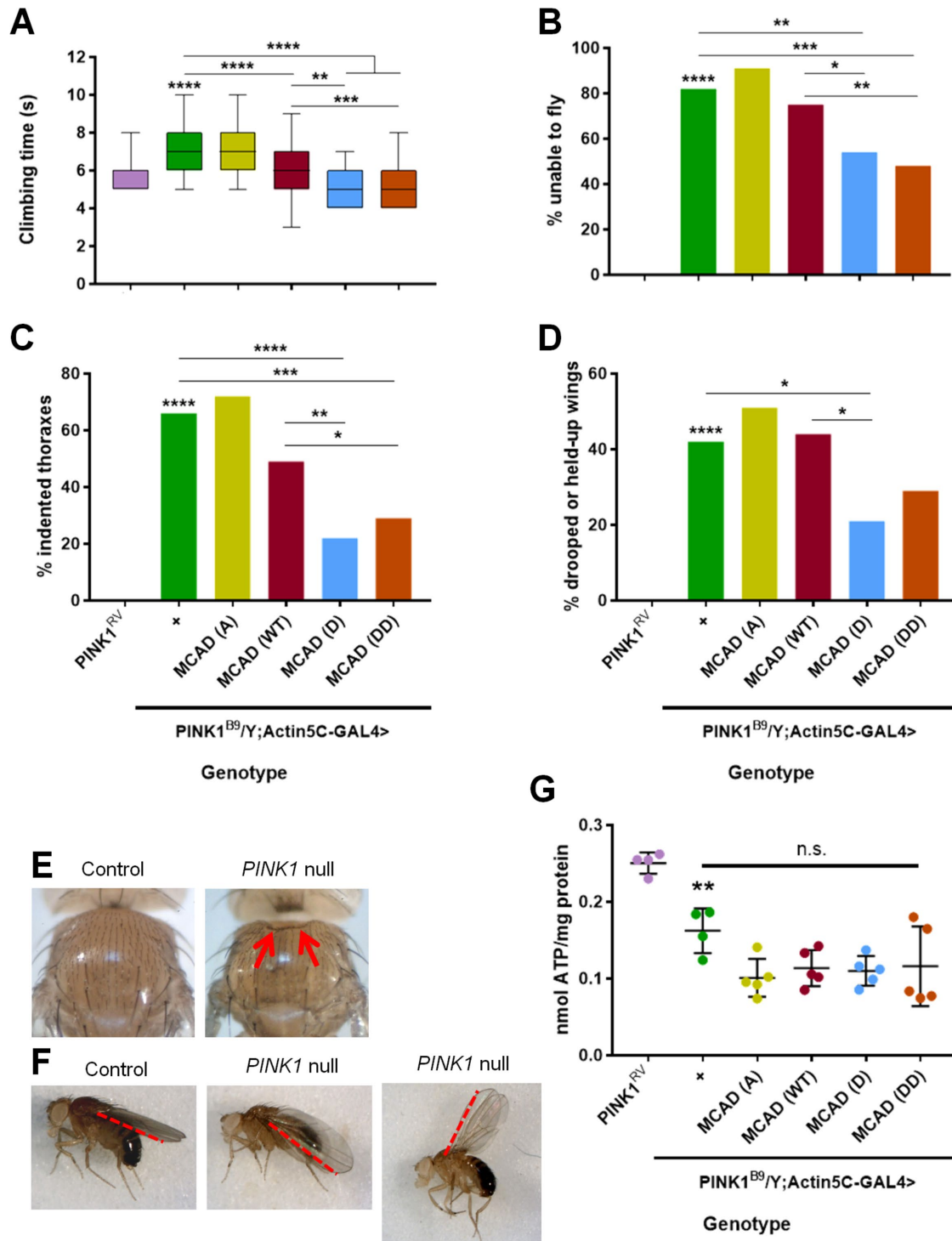
FIGURE 2: Phosphomimetic MCAD S347 rescues *PINK1* null phenotypes. (A–F) All assays were conducted in 3- to 4-d-old male flies. *n* = 50–55 flies. For all panels, comparison is to *PINK1*[RV] unless otherwise indicated. All lines showing significance represent two-group comparisons. *$p < 0.05$, **$p < 0.01$, ***$p < 0.001$, ****$p < 0.0001$ for all figures. (A) Time flies take to climb upward 8 cm. One-way ANOVA, followed by Tukey's multiple comparisons. Middle line is the median, outer edges of the box are 25th and 75th percentiles, and whiskers are the minimum and maximum values. (B) Percentage of flies that cannot fly. (C) Percentage of flies with indented thoraxes. (D) Percentage of flies with drooped or held-up wings. (B–D) Chi-square test, followed by Fisher's exact tests. (E) Representative images of a healthy *PINK1*[RV] (control) thorax (left), and the indented thorax of a *PINK1*[B9] (null) fly (right). Red arrows indicate indentation. (F) Representative images of healthy *PINK1*[RV] wings (left), as well as drooped (middle) and held-up (right) wings in *PINK1*[B9] flies. Red dotted lines emphasize the varying angles of the wings. (G) ATP levels divided by total protein levels, *n* = 4–5 samples, four flies per sample. One-way ANOVA, followed by Tukey's multiple comparisons; n.s., not significant.

MCAD's rescue of *PINK1* null flies is independent of ATP production

Mitochondrial ATP production is compromised in *PINK1* null flies, and is also influenced by MCAD enzymatic activity (Clark *et al.*, 2006; Park *et al.*, 2006; Vilain *et al.*, 2012; Vos *et al.*, 2012, 2017; Houten *et al.*, 2016), so we tested whether MCAD (D)/(DD) restores *PINK1* null's organismal phenotypes by improving mitochondrial ATP generation. We found that neither MCAD (D) nor (DD) rescued the ATP deficit in *PINK1* null flies, and that their ATP levels were indistinguishable from those of MCAD (A) and (WT) (Figure 2G). Therefore, it is likely that MCAD (D)/(DD) promotes mitochondrial functions other than ATP production to rescue *PINK1* null's organismal phenotypes.

MCAD's rescue of *PINK1* null flies is independent of its conventional role in β-oxidation

We next asked whether the observed organismal rescue could be due to MCAD's role in β-oxidation. To answer this question, we analyzed the flies' acylcarnitine profiles. This profile analysis is a well-established method by which newborns and patients are tested for defects in fatty acid oxidation, including MCAD enzymatic deficiency (Rinaldo *et al.*, 2008). In addition to *PINK1* null flies and their controls, we assayed MCAD deficient flies to validate that this analysis works in flies as it does in humans. Because there was no MCAD knockout fly available, we generated a fly model of MCAD deficiency by deleting a ~1.5 kb fragment of the *MCAD* gene using CRISPR/Cas9 (Gratz *et al.*, 2013), which we will call *MCAD*^*mut*^. We also drove a UAS-MCAD RNAi line with Tubulin-GAL4 as an MCAD knockdown (Supplemental Figure S4A). Our homozygous *MCAD*^*mut*^, transheterozygous *MCAD*^*mut*^ over a deficiency (Df) locus covering *MCAD*, and ubiquitous *MCAD* RNAi flies all exhibited significant elevations in medium-chain acylcarnitines characteristic of human MCAD deficiency: C6, C8, and C10:1 acylcarnitines. As expected, this pattern was exacerbated by starvation, because lowered glucose levels promote fatty acid oxidation (Houten *et al.*, 2016). The elevations observed in *MCAD*^*mut*^ flies were fully rescued by expression of MCAD (WT), confirming that these elevations were specifically due to lack of MCAD (Figure 3). This profile is, to our knowledge, the first time that fly MCAD deficiency has been tested for similarity to human MCAD deficiency and validates our protocol.

We did not find that *PINK1* null flies exhibited the same, stereotypical MCAD deficiency. Although C6 and C8 acylcarnitines increased slightly under both fed and starved conditions, their increase was nominal compared with the remarkable elevations observed in MCAD deficient flies (Figure 3, inset). Additionally, *PINK1* null flies did not exhibit a significant C10:1 acylcarnitine increase (Figure 3 and Supplemental Table S2), suggesting that MCAD is still enzymatically active as an acyl-CoA dehydrogenase in *PINK1* null flies. Expression of MCAD (D)/(DD) in *PINK1* null flies did not alter their acylcarnitine profiles (Supplemental Figure S5). Therefore, phosphomimetic MCAD S347 likely rescues *PINK1* null's organismal phenotypes independently of MCAD's acyl-CoA dehydrogenase activity.

PINK1 null flies have acylcarnitine and amino acid disruptions, which are selectively rescued by phosphomimetic MCAD S347

In addition to MCAD enzymatic deficiency, we used our acylcarnitine profile to determine whether other parts of the fatty acid oxidation pathway were affected by loss of PINK1. Our *PINK1* null flies showed significant decreases in free carnitine and C2 and C3 acylcarnitines. In addition to C6 and C8 acylcarnitine (Figure 3, A and B), *PINK1* null flies showed significant increases in four medium-chain acylcarnitines (whose elevations are not prominent characteristics of traditional MCAD deficiency), as well as nine long-chain acylcarnitines (Supplemental Table S2). Owing to increasing evidence that *PINK1* plays a role in lipid and amino acid metabolic homeostasis (Senyilmaz *et al.*, 2015; Stauch *et al.*, 2016; Vos *et al.*, 2017), we also measured free amino acids in *PINK1* null flies. Of 40 amino acids tested, the flies were significantly deficient in 10 and had elevations in five (Supplemental Table S3).

After identifying metabolites that were altered in *PINK1* null flies, we wanted to know which might be involved in MCAD's rescue of *PINK1* null's phenotypes. Among the metabolite deficiencies we observed in *PINK1* null flies were C3 acylcarnitine, β-alanine, and arginine, which were rescued by expression of our phosphomimetic MCAD, as compared with our phosphoresistant MCAD. Similarly, two metabolites that were significantly elevated in *PINK1* null flies were lysine and argininosuccininc acid, which were rescued by expression of our phosphomimetic MCAD, as compared with our phosphoresistant MCAD (Figure 4). Because the rescue of these metabolites by phosphomimetic MCAD are consistent with the rescue of *PINK1* null's flight, climbing, thorax, and wing posture phenotypes, phosphorylation of MCAD S347 may restore *PINK1* null's organismal function in part by restoring these acylcarnitine and amino acid abnormalities.

DISCUSSION

In this study, we found that the phosphorylation of MCAD at site S347 is dependent on PINK1 and that mimicking phosphorylation at this site in *PINK1* null flies can rescue their flight, climbing, thorax, and wing posture phenotypes. To better understand why this phosphorylation is beneficial, we examined canonical functions of PINK1 and MCAD and found that the mechanism of rescue is divorced from both PINK1's role in ATP generation, as well as MCAD's role in β-oxidation. Instead, mimicking phosphorylation of MCAD S347 in a *PINK1* null background corresponds to rescuing the altered C3 acylcarnitine, β alanine, arginine, lysine, and argininosuccininc acid levels found in *PINK1* null flies. In addition, we established the first MCAD deficiency fly model and identified significant metabolite alterations in *PINK1* null flies: 15 amino acids belonging to numerous metabolic pathways and 17 acylcarnitines of widely varying chain lengths. Thus, PINK1 plays a role in fatty acid and amino acid metabolism and mediates a novel function of the β-oxidation enzyme MCAD.

Our findings validate and expand on PINK1's role in metabolic homeostasis, revealing a sweeping array of amino acids and acylcarnitines affected. While *PINK1* null flies likely do not have an MCAD enzymatic deficiency, their acylcarnitine profiles reveal other β-oxidation defects. The pattern of disrupted short-, medium-, and long-chain acylcarnitines is suggestive of multiple acyl-CoA dehydrogenase deficiency (MADD) and does share some similarities to a MADD fly model (Alves *et al.*, 2012). *PINK1* knockout rats also show significantly decreased levels of both α and β subunits of electron transfer flavoprotein (ETF), which is consistent with our finding, since disruption of either of these subunits is a cause of MADD (Stauch *et al.*, 2016). The elevations in long-chain acylcarnitines are particularly notable, and prominent peaks at C16 and C18:1 acylcarnitines are reminiscent of those found in human deficiencies in carnitine palmitoyltransferase 2 (CPT2) and/or carnitine acyl-CoA translocase (CACT). This observation is consistent with the recent finding that *PINK1* knockout rats show significantly decreased levels of CPT2, as well as the finding that decreased
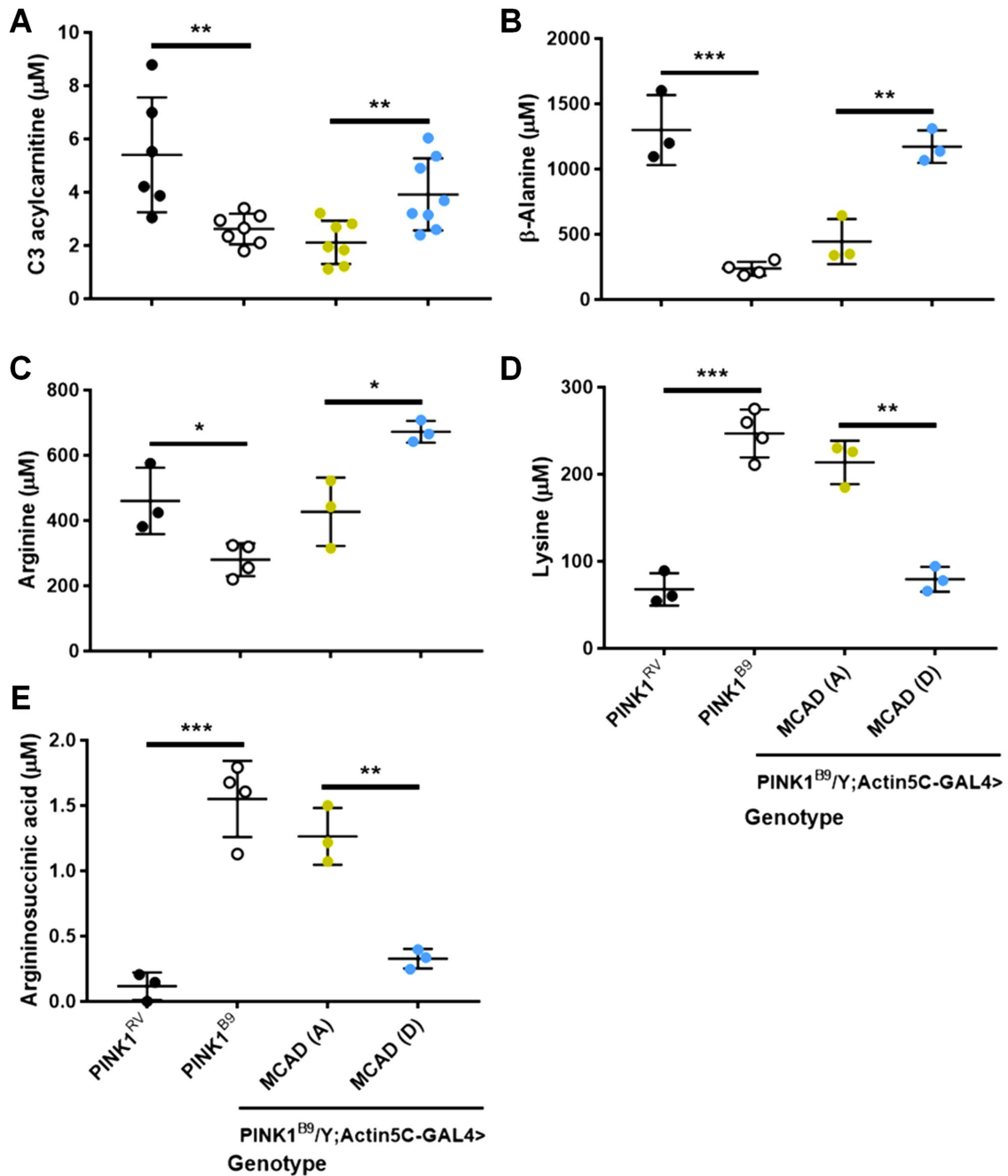
FIGURE 3: Acylcarnitine analysis in *PINK1* null and *MCAD* mutant flies. Acylcarnitine analysis in lysates from 6- to 7-d-old male flies. "Starved" condition means flies were switched to vials containing only water for the final 24 h. Student's *t* tests, *n* = 3–10 samples, five flies per sample, two technical replicates averaged per sample. Abundance of (A) C6, (B) C8, and (C) C10:1 acylcarnitines in MCAD deficient flies and *PINK1* null flies.

PINK1 protein levels correlate to decreased very long-chain acyl-CoA dehydrogenase (VLCAD) levels in human brains (Choi *et al.*, 2014; Stauch *et al.*, 2016). Both of these deficiencies could lead to the elevations in long-chain acylcarnitines that we observed. The free amino acids disrupted in *PINK1* null flies are wide-ranging and include essential, nonessential, and conditional amino acids. Because recent research in the *PINK1* field indicates the need for more thorough metabolic analysis (Senyilmaz *et al.*, 2015; Vos *et al.*, 2017), our methods and results provide a template for future validation.

FIGURE 4: MCAD S347D selectively rescues *PINK1* null's acylcarnitine and amino acid deficiencies. Comparing selected acylcarnitines and amino acids between *PINK1^RV^* and *PINK1^B9^*, and *PINK1^B9^*; *Actin5C-GAL4>MCAD (A)* and *PINK1^B9^*; *Actin5C-GAL4>MCAD (D)*. Student's *t* tests, *n* = 3–8 samples, five flies per sample, two technical replicates averaged per sample.

In the process of developing our metabolic profiles, we generated the first MCAD deficiency fly model, confirmed the canonical role of *Drosophila* MCAD in medium-chain fatty acid β-oxidation, and established that the fly MCAD deficiency acylcarnitine profile looks strikingly similar to the human profile, suggesting that the fly could be a good model for studying this and other inborn errors of metabolism. We also identified a new role for MCAD through PINK1-mediated phosphorylation of S347, since it rescues *PINK1* null's disruptions in C3 acylcarnitine, β alanine, arginine, lysine, and argininosuccininc acid without rescuing its dehydrogenase activity.

These final three amino acids are metabolically linked in that argininosuccinic acid is a precursor of arginine, and arginine and lysine compete for the same transport proteins. Because we found that some fly MCAD localizes to the cytosol (Figure 1E), and PINK1 has been recently reported to have kinase activity there (Lee *et al.*, 2017), there are several possibilities as to where PINK1 and MCAD interact and influence downstream targets. Phosphorylation of MCAD at S347 could cause a conformational change or alter protein binding to influence amino acids and acylcarnitines nearby or trigger a long-range signal to affect other metabolic pathways.

Because we assayed the *PINK1* null flies under physiological conditions, we have further expanded PINK1's role beyond stress-induced mitophagy. As fly and human PINK1 are functionally conserved (Clark *et al.*, 2006), our observations of PINK1's role in fly metabolic homeostasis could be relevant to human PINK1 as well. Recessive mutations in human *PINK1* cause Parkinson's disease, which is the second most common neurodegenerative disorder, as well as the second most common movement disorder. This study suggests that metabolic imbalance may constitute a part of pathogenesis in human neurodegenerative diseases.

Metabolism is a keystone of cellular function and must be tightly controlled, especially in cells with high energy demands. Our work links PINK1 to the β-oxidation enzyme MCAD and to lipid and amino acid metabolism and is one example of how metabolic profiling can be a rapid and effective way to study molecular and cellular functions of disease-causing genes. It also serves as a reminder of the underappreciated roles of known enzymes in metabolic activity and illustrates the power of coupling metabolic profiling with *Drosophila* genetics to identify those roles.

MATERIALS AND METHODS

Fly stocks
Fly stocks used were *PE704*, *PINK1⁵* (Clark *et al.*, 2006), *PINK1^{RV}*, *PINK1^{B9}* (Park *et al.*, 2006), *Actin5C-GAL4*, *Tubulin-GAL4*, *UAS-MCAD RNAi^{KK}* (VDRC 107820), *y¹ v¹; P{CaryP}attP40* (BDSC 36304), *M{vas-Cas9}ZH-2A* (BDSC 51323), and *Df(3L)BSC631* (BDSC 25722). All flies were maintained at 25°C and flipped into new food every 3–4 d. For details on the creation of transgenic flies and use of CRISPR/Cas9, please see the Supplemental Experimental Procedures.

Western blots and kinase assay
Please see the Supplemental Experimental Procedures.

Behavioral assays
To assess climbing ability, 3- to 4-d-old male flies were placed in a vial one at a time, allowed to acclimate for 1 min, gently tapped to the bottom, and then the time the fly took to climb 8 cm was recorded. To assess flight ability, flies were tapped one at a time out of a vial held upside down 1 ft over a bench top. If the fly flew away, then it was recorded as "1," and if it was unable to fly, then it was recorded as "0."

Wing and thorax assays
Wing posture was assessed in 3- to 4-d-old male flies by viewing a vial of five flies each under a dissecting scope, and recording whether wings were held normally ("0") or drooped or held-up ("1"). Thorax indentations were observed by placing flies on a CO_2 pad and viewing their thoraxes under a dissecting microscope. A healthy thorax was recorded as "0," while an indented thorax was recorded as "1."

ATP determination
ATP levels from lysates of four 30- to 31-d-old male flies per sample were measured using an ATP Determination Kit (Molecular Probes A22066). Flies were homogenized in 100 µl lysis buffer (6M guanidine-HCL, 100 mM Tris, 4 mM EDTA, pH 7.8 [Park *et al.*, 2006]), boiled for 5 min, placed on ice for 5 min, and centrifuged at 17,000 × *g* for 15 min. The supernatant was diluted 1:500 with kit reaction buffer, luciferase was added for 3 min, and then luminescence was measured on a GloMax Jr. luminometer (Promega). Values were normalized to protein levels, which were determined by diluting samples 1:1 and using a BCA Protein Assay Kit (Pierce 23225).

Phosphopeptide, acylcarnitine, and amino acid analysis
Please see the Supplemental Experimental Procedures.

Statistical analysis
Statistical analyses were performed using GraphPad Prism 7.03. To first confirm that the data were normally distributed, the D'Agostino-Pearson omnibus K2 test was used for $N \geq 8$, and the Shapiro–Wilk test was used if $N < 8$. Student's *t* tests were used to compare groups of two with Gaussian distributions. One-way analyses of variance (ANOVAs) were used to compare groups greater than two with Gaussian distributions, followed by Tukey's multiple comparisons tests if the ANOVA gave $p < 0.05$. A chi-square test was used on groups of binary data, followed by Fisher's exact tests if the chi-square gave $p < 0.05$.

REFERENCES
Alves E, Henriques BJ, Rodrigues JV, Prudêncio P, Rocha H, Vilarinho L, Martinho RG, Gomes CM (2012). Mutations at the flavin binding site of ETF: QO yield a MADD-like severe phenotype in *Drosophila*. Biochim Biophys Acta 1822, 1284–1292.

Bian Y, Song C, Cheng K, Dong M, Wang F, Huang J, Sun D, Wang L, Ye M, Zou H (2014). An enzyme assisted RP-RPLC approach for in-depth analysis of human liver phosphoproteome. J Proteomics 96, 253–262.

Bischof J, Maeda RK, Hediger M, Karch F, Basler K (2007). An optimized transgenesis system for Drosophila using germ-line-specific C31 integrases. Proc Natl Acad Sci USA 104, 3312–3317.

Brand AH, Perrimon N (1993). Targeted gene expression as a means of altering cell fates and generating dominant phenotypes. Development 118, 401–415.

Chen Y, Dorn GW (2013). PINK1-Phosphorylated mitofusin 2 is a Parkin receptor for culling damaged mitochondria. Science 340, 471–476.

Choi J, Ravipati A, Nimmagadda V, Schubert M, Castellani RJ, Russell JW (2014). Potential roles of PINK1 for increased PGC-1α-mediated mitochondrial fatty acid oxidation and their associations with Alzheimer disease and diabetes. Mitochondrion 18, 41–48.

Clark IE, Dodson MW, Jiang C, Cao JH, Huh JR, Seol JH, Yoo SJ, Hay BA, Guo M (2006). Drosophila pink1 is required for mitochondrial function and interacts genetically with parkin. Nature 441, 1162–1166.

Du J, Li Z, Li QZ, Guan T, Yang Q, Xu H, Pritchard KA, Camara AK, Shi Y (2013). Enoyl coenzyme A hydratase domain-containing 2, a potential novel regulator of myocardial ischemia injury. J Am Heart Assoc 2, e000233.

Gehrke S, Wu Z, Klinkenberg M, Sun Y, Auburger G, Guo S, Lu B (2015). PINK1 and Parkin control localized translation of respiratory chain component mRNAs on mitochondria outer membrane. Cell Metab 28, 1304–1314.

Geisler S, Holmström KM, Skujat D, Fiesel FC, Rothfuss OC, Kahle PJ, Springer W (2010). PINK1/Parkin-mediated mitophagy is dependent on VDAC1 and p62/SQSTM1. Nat Cell Biol 12, 119–131.

Gratz SJ, Cummings AM, Nguyen JN, Hamm DC, Donohue LK, Harrison MM, Wildonger J, O'Connor-Giles KM (2013). Genome engineering of Drosophila with the CRISPR RNA-guided Cas9 nuclease. Genetics 194, 1029–1035.

Grimsrud PA, Carson JJ, Hebert AS, Hubler SL, Niemi NM, Bailey DJ, Jochem A, Stapleton DS, Keller MP, Westphall MS, *et al.* (2012). A quantitative map of the liver mitochondrial phosphoproteome reveals posttranslational control of ketogenesis. Cell Metab 16, 672–683.

Houten SM, Violante S, Ventura FV, Wanders RJA (2016). The biochemistry and physiology of mitochondrial fatty acid β-oxidation and its genetic disorders. Annu Rev Physiol 78, 23–44.

Humphrey SJ, Yang G, Yang P, Fazakerley DJ, Stöckli J, Yang JY, James DE (2013). Dynamic adipocyte phosphoproteome reveals that akt directly regulates mTORC2. Cell Metab 17, 1009–1020.

Kane LA, Lazarou M, Fogel AI, Li Y, Yamano K, Sarraf SA, Banerjee S, Youle RJ (2014). PINK1 phosphorylates ubiquitin to activate parkin E3 ubiquitin ligase activity. J Cell Biol 205, 143–153.

Kazlauskaite A, Kondapalli C, Gourlay R, Campbell DG, Ritorto MS, Hofmann K, Alessi DR, Knebel A, Trost M, Muqit MMK (2014). Parkin is activated by PINK1-dependent phosphorylation of ubiquitin at Ser[65]. Biochem J 460, 127–141.

Kondapalli C, Kazlauskaite A, Zhang N, Woodroof HI, Campbell DG, Gourlay R, Burchell L, Walden H, Macartney TJ, Deak M, *et al.* (2012). PINK1 is activated by mitochondrial membrane potential depolarization and stimulates Parkin E3 ligase activity by phosphorylating serine 65. Open Biol 2, 120080.

Koyano F, Okatsu K, Kosako H, Tamura Y, Go E, Kimura M, Kimura Y, Tsuchiya H, Yoshihara H, Hirokawa T, *et al.* (2014). Ubiquitin is phosphorylated by PINK1 to activate parkin. Nature 510, 162–166.

Lee Y, Stevens DA, Kang S, Dawson VL, Shin J, Dawson TM (2017). PINK1 primes Parkin-mediated ubiquitination of PARIS in dopaminergic neuronal survival. Cell Rep 18, 918–932.

Liu W, Acín-Peréz R, Geghman KD, Manfredi G, Lu B, Li C (2011). Pink1 regulates the oxidative phosphorylation machinery via mitochondrial fission. Proc Natl Acad Sci USA 108, 12920–12924.

Markstein M, Pitsouli C, Villalta C, Celniker SE, Perrimon N (2008). Exploiting position effects and the gypsy retrovirus insulator to engineer precisely expressed transgenes. Nat Genet 40, 476–483.

Morais VA, Haddad D, Craessaerts K, Bock P De, Swerts J, Vilain S, Aerts L, Overbergh L, Seibler P, Klein C, *et al.* (2014). PINK1 loss-of-function mutations affect mitochondrial complex I activity via NdufA10 ubiquinone uncoupling. Science 431, 203–208.

Mulhern D (2012). CST Curation Set: 13828; Year: 2012; biosample/treatment: cell line, Jurkat/calyculin_A & pervanadate; disease: T cell leukemia; SILAC: -; specificities of antibodies used to purify peptides prior to LCMS: (K/R)XpSX(K/R).

Narendra D, Tanaka A, Suen D-F, Youle RJ (2008). Parkin is recruited selectively to impaired mitochondria and promotes their autophagy. J Cell Biol 183, 795–803.

Narendra DP, Jin SM, Tanaka A, Suen D-F, Gautier CA, Shen J, Cookson MR, Youle RJ (2010). PINK1 is selectively stabilized on impaired mitochondria to activate Parkin. PLoS Biol 8, e1000298.

Park J, Lee SB, Lee S, Kim Y, Song S, Kim S, Bae E, Kim J, Shong M, Kim J-M, *et al.* (2006). Mitochondrial dysfunction in Drosophila PINK1 mutants is complemented by parkin. Nature 441, 1157–1161.

Pearlman SM, Serber Z, Ferrell JE (2011). A mechanism for the evolution of phosphorylation sites. Cell 147, 934–946.

Pogson JH, Ivatt RM, Sanchez-martinez A, Tufi R, Wilson E, Mortiboys H, Whitworth AJ (2014). The complex I subunit NDUFA10 selectively rescues Drosophila pink1 mutants through a mechanism independent of mitophagy. PLoS Genet 10, e1004815.

Poole AC, Thomas RE, Andrews LA, McBride HM, Whitworth AJ, Pallanck LJ (2008). The PINK1/Parkin pathway regulates mitochondrial morphology. Proc Natl Acad Sci USA 105, 1638–1643.

Poole AC, Thomas RE, Yu S, Vincow ES, Pallanck L (2010). The mitochondrial fusion-promoting factor mitofusin is a substrate of the PINK1/Parkin pathway. PLoS One 5, e10054.

Possemato A (2010). CST Curation Set: 9289; Year: 2010; biosample/treatment: cell line, Jurkat/pervanadate; disease: T cell leukemia; SILAC: -; specificities of antibodies used to purify peptides prior to LCMS: pTXR.

Rinaldo P, Cowan TM, Matern D (2008). Acylcarnitine profile analysis. Genet. Med 10, 151–156.

Rinaldo P, Matern D, Bennett MJ (2002). Fatty acid oxidation disorders. Annu Rev Physiol 64, 477–502.

Senyilmaz D, Virtue S, Xu X, Tan CY, Griffin JL, Miller AK, Vidal-Puig A, Teleman AA (2015). Regulation of mitochondrial morphology and function by stearoylation of TFR1. Nature 525, 124–128.

Stauch KL, Villeneuve LM, Purnell PR, Ottemann BM, Emanuel K, Fox HS (2016). Loss of Pink1 modulates synaptic mitochondrial bioenergetics in the rat striatum prior to motor symptoms: concomitant complex I respiratory defects and increased complex II-mediated respiration. Proteomics Clin Appl 10, 1205–1217.

Strickfaden SC, Winters MJ, Ben-Ari G, Lamson RE, Tyers M, Pryciak PM (2007). A mechanism for cell-cycle regulation of MAP kinase signaling in a yeast differentiation pathway. Cell 128, 519–531.

Tanaka A, Cleland MM, Xu S, Narendra DP, Suen DF, Karbowski M, Youle RJ (2010). Proteasome and p97 mediate mitophagy and degradation of mitofusins induced by Parkin. J Cell Biol 191, 1367–1380.

Valente EM, Abou-Sleiman PM, Caputo V, Muqit MMK, Harvey K, Gispert S, Ali Z, Del Turco D, Bentivoglio AR, Healy DG, *et al.* (2004a). Hereditary early-onset Parkinson's disease caused by mutations in PINK1. Science 304, 1158–1160.

Valente EM, Salvi S, Ialongo T, Marongiu R, Elia AE, Caputo V, Romito L, Albanese A, Dallapiccola B, Bentivoglio AR (2004b). PINK1 mutations are associated with sporadic early-onset parkinsonism. Ann Neurol 56, 336–341.

Vilain S, Esposito G, Haddad D, Schaap O, Dobreva MP, Vos M, Van Meensel S, Morais VA, De Strooper B, Verstreken P (2012). The yeast complex I equivalent NADH dehydrogenase rescues pink1 mutants. PLoS Genet 8, e1002456.

Vives-Bauza C, Przedborski S (2011). Mitophagy: the latest problem for Parkinson's disease. Trends Mol Med 17, 158–165.

Vos M, Esposito G, Edirisinghe JN, Vilain S, Haddad DM, Slabbaert JR, Van Meensel S, Schaap O, De Strooper B, Meganathan R, *et al.* (2012). Vitamin K2 is a mitochondrial electron carrier that rescues pink1 deficiency. Science 336, 1306–1310.

Vos M, Geens A, Böhm C, Deaulmerie L, Swerts J, Rossi M, Craessaerts K, Leites EP, Seibler P, Rakovic A, *et al.* (2017). Cardiolipin promotes electron transport between ubiquinone and complex I to rescue PINK1 deficiency. J Cell Biol 216, 695–708.

Wang X, Winter D, Ashrafi G, Schlehe J, Wong YL, Selkoe D, Rice S, Steen J, LaVoie MJ, Schwarz TL (2011). PINK1 and Parkin target Miro for phosphorylation and degradation to arrest mitochondrial motility. Cell 147, 893–906.

Whitworth AJ, Pallanck LJ (2009). The PINK1/Parkin pathway: a mitochondrial quality control system? J Bioenerg Biomembr 41, 499–503.

Whitworth AJ, Pallanck LJ (2017). PINK1/Parkin mitophagy and neurodegeneration—what do we really know in vivo? Curr Opin Genet Dev 44, 47–53.

Woodroof HI, Pogson JH, Begley M, Cantley C, Deak M, Campbell DG, Van DMF, Whitworth AJ, Alessi DR, Muqit MK (2011). Discovery of catalytically active orthologues of the Parkinson's disease kinase PINK1: analysis of substrate specificity and impact of mutations. Open Biol 1, 110012.

Wu G (2009). Amino acids: metabolism, functions, and nutrition. Amino Acids 37, 1–17.

Yang Y, Gehrke S, Imai Y, Huang Z, Ouyang Y, Wang J-W, Yang L, Beal MF, Vogel H, Lu B (2006). Mitochondrial pathology and muscle and dopaminergic neuron degeneration caused by inactivation of Drosophila Pink1 is rescued by Parkin. Proc Natl Acad Sci USA 103, 10793–10798.

Yang Y, Ouyang Y, Yang L, Beal MF, McQuibban A, Vogel H, Lu B (2008). Pink1 regulates mitochondrial dynamics through interaction with the fission/fusion machinery. Proc Natl Acad Sci USA 105, 7070–7075.

Zhou C, Huang Y, Shao Y, May J, Prou D, Perier C, Dauer W, Schon EA, Przedborski S (2008). The kinase domain of mitochondrial PINK1 faces the cytoplasm. Proc Natl Acad Sci USA 105, 12022–12027.

Ziviani E, Tao RN, Whitworth AJ (2010). Drosophila Parkin requires PINK1 for mitochondrial translocation and ubiquitinates Mitofusin. Proc Natl Acad Sci USA 107, 5018–5023.